

The 2-3 mixing and mass split: atmospheric neutrinos and magnetized spectrometers

Abhijit Samanta^{a,b} and A. Yu. Smirnov^b

^a*Ramakrishna Mission Vivekananda University, Belur Math, Howrah 711 202, India*

^b*The Abdus Salam International Centre for Theoretical Physics
Strada Costiera 11, I-34014 Trieste, Italy*

We study dependence of the atmospheric ν_μ and $\bar{\nu}_\mu$ fluxes on the deviations of the 2-3 mixing from maximal, $|45^\circ - \theta_{23}|$, on the θ_{23} -octant and on the neutrino mass splitting Δm_{32}^2 . Analytic expressions for the θ_{23} -deviation effect and the octant asymmetry are derived. We present conservative estimations of sensitivities of the iron (magnetized) calorimeter detectors (ICAL) to these parameters. ICAL can establish the θ_{23} -deviation at higher than 3σ confidence level if $|45^\circ - \theta_{23}| > 6^\circ$ with the exposure of 1 Mton-yr. Sensitivity to the octant is low for zero or very small 1-3 mixing, but it can be substantially enhanced for $\theta_{13} > 3^\circ$. ICAL can measure the difference of Δm_{32}^2 in ν and $\bar{\nu}$ channels (the CPT test) with accuracy $0.8 \times 10^{-4} \text{ eV}^2$ (3σ) with 1 Mton-yr exposure, and the present MINOS result can be excluded at $> 5\sigma$ confidence level. We discuss possible ways to further improve sensitivity of the magnetized spectrometers.

PACS numbers: 14.60.Pq, 14.60.Lm

I. INTRODUCTION

Determination of the 2-3 mass splitting and leptonic mixing, and in particular, the deviation of θ_{23} from the maximal mixing angle,

$$\delta_{23} \equiv 45^\circ - \theta_{23}, \quad (1)$$

is of fundamental importance¹. Here we use the standard parameterization of the PMNS mixing matrix:

$$U_{PMNS} = U_{23}(\theta_{23})\Gamma_\delta U_{13}(\theta_{13})U_{12}(\theta_{12}), \quad (2)$$

where U_{ij} is the matrix of rotation in the ij -plane, and $\Gamma_\delta \equiv \text{diag}(0, 0, e^{i\delta})$. Being maximal or close to maximal, the 2-3 mixing testifies for existence of certain underlying symmetry [1]. Comparison of the values of δ_{23} and θ_{13} as well as the mixing angles in the quarks and lepton sectors can shed some light on the origins of fermion mass and mixing in general.

The existing results on θ_{23} and Δm_{23}^2 are summarized in the Table 1. Note that the global fits of oscillation data [2] (see also [3]) show some deviation of the 2-3 mixing from maximal: $\delta_{23} = 2 - 3^\circ$ (1σ). Although the data agree well with maximal mixing, large deviation, $\delta_{23} = \pm 9^\circ$, is still possible.

Concerning the 2-3 mass splitting, the global fit values are in agreement with the results of SuperKamiokande (SK) [4] as well as the MINOS measurement in the ν channel [5].

Recently MINOS has reported the values of Δm_{31}^2 and θ_{23} in the $\bar{\nu}$ channel [5] which differ from those in the ν channel (see tables I and II). If confirmed, this result will testify for an effective (due to existence of some new interactions [6]) or fundamental CPT violation. The analysis of the atmospheric neutrino data does not confirm MINOS result although the sensitivity of SK to CPT violation is not high since SK sum up effects of neutrinos and antineutrinos [6]. Iron calorimeters (ICAL) [7] can perform very sensitive search for the CPT violation and check MINOS result.

New accelerator experiments T2K [8] and NO ν A [9] will improve precision of measurements of Δm_{32}^2 by factor 2, but their accuracy of measurements of θ_{23} will be only slightly better than that of the present global fit (see table I).

There are two aspects of the θ_{23} -measurements:

- determination of the absolute value of the deviation $|\delta_{23}|$, and
- identification of the θ_{23} -octant, *i.e.* the sign of δ_{23} , or in other words, resolution of the octant degeneracy.

The problem of determination of δ_{23} and the octant with atmospheric neutrinos has been addressed in a number of publications before [10–16]. It was realized [11–13] that at low energies oscillation effects on the electron neutrino flux are proportional to this deviation, and therefore searches for an excess (or suppression) of events in the sub-GeV range would testify for δ_{23} . For water Cherenkov detectors both aspects of the 2-3 mixing determinations have been explored

¹ δ_{23} is related to another deviation parameter, $D_{23} \equiv 1/2 - \sin^2 \theta_{23}$ used in literature as $D_{23} = \sin 2\delta_{23}$.

in [12, 13]. The study was mainly concentrated on effects in the electron neutrino flux.

Magnetized calorimeters are mainly aimed at a detection of the muon neutrinos, but they can distinguish neutrinos and antineutrinos, and this composes their main advantage. These detectors provide better energy and angular resolution of the charged leptons, and consequently, neutrinos. A possibility to disentangle neutrinos and antineutrinos reinforces the following features: i) The energy and angular resolutions (reconstruction) are different for neutrinos and antineutrinos. ii) Sensitivities of the neutrino and antineutrino channels to the oscillation parameters are substantially different.

Sensitivity of a magnetized calorimeter to the 2-3 mixing and mass splitting has been explored in [14] and [15]. It has been shown that at nonzero value of the 1-3 mixing the octant discrimination is more feasible with the magnetized detector than with the water Cherenkov detector since the former can directly measure the matter effect [14]. In these studies, however, various simplifications have been made which do not allow for realistic estimations of potential of the experiments. In the analysis [17] a possibility of the octant discrimination has been evaluated for two benchmark values of θ_{23} and relatively high $\theta_{13} = 7.5^\circ$.

Here we present a comprehensive study of sensitivities of the ICAL to the parameters of 2-3 sector. We assume that by the time of operation of this detector certain information about θ_{13} will be obtained.

The paper is organized as follows. In sec. II we study dependence of the ν_μ and $\bar{\nu}_\mu$ fluxes on parameters of the 2-3 sector: $|\delta_{23}|$, octant and Δm_{23}^2 . In sec. III we describe details of our statistical analysis. We evaluate physics potential of the magnetized calorimeter to measure these parameters in sec. IV. In sec. V we consider further improvements of sensitivities of the magnetized calorimeters. Conclusions are given in sec. VI.

II. DEPENDENCE OF THE ATMOSPHERIC NEUTRINO FLUXES ON 2-3 MIXING

The original atmospheric neutrino flux contains both the muon, F_μ^0 , and electron, F_e^0 , neutrino components, so that the muon neutrino flux at a detector equals

$$\begin{aligned} F_\mu &= F_\mu^0 P_{\nu_\mu \rightarrow \nu_\mu} + F_e^0 P_{\nu_e \rightarrow \nu_\mu} \\ &= F_\mu^0 \left[P_{\nu_\mu \rightarrow \nu_\mu} + \frac{1}{r} P_{\nu_e \rightarrow \nu_\mu} \right]. \end{aligned} \quad (3)$$

Here the flavor ratio

$$r(E, \theta_Z) \equiv \frac{F_\mu^0(E, \theta_Z)}{F_e^0(E, \theta_Z)} \quad (4)$$

is function of the neutrino energy E and zenith angle θ_Z .

For the standard parameterization of the mixing matrix dependence of the oscillation probabilities on the 2-3 mixing θ_{23} and CP-phase δ is *explicit* for an arbitrary density profile. This follows from the order of rotation in eq. (2) and the fact that the matrix of matter potentials has the form $V = \text{diag}\{V_e, 0, 0\}$ in the flavor basis, *i.e.* it is invariant under the 2-3 rotations. Indeed, the neutrino evolution can be considered in the propagation basis, $\tilde{\nu} \equiv (\nu_e, \tilde{\nu}_2, \tilde{\nu}_3)$, defined via the following relation with the flavor basis: $\nu_f \equiv U_{23} \Gamma_\delta \tilde{\nu}$. Consequently, $\tilde{\nu} = U_{13} U_{12} \nu_{mass}$, where $\nu_{mass} \equiv (\nu_1, \nu_2, \nu_3)$ is the basis of mass eigenstates. In the propagation basis the Hamiltonian, and therefore the amplitudes of transitions depend on $\theta_{13}, \theta_{12}, V_e$, and mass squared differences:

$$A_{\alpha\beta} = A_{\nu_\alpha \rightarrow \nu_\beta}(\theta_{13}, \theta_{12}, V_e), \quad \alpha, \beta = e, \tilde{2}, \tilde{3}, \quad (5)$$

and they do not depend on θ_{23} and δ . In the flavor basis, dependence of the amplitudes A_f on these parameters appears via projections of the matrix of amplitudes (5) from the propagation basis to the flavor basis:

$$\hat{A}_f = U_{23} \Gamma_\delta \hat{A} \Gamma_{-\delta} U_{23}^T, \quad (6)$$

where \hat{A}^f is the matrix of amplitudes in the flavor basis.

In terms of the amplitudes $A_{\alpha\beta}$ using eq. (6) one can rewrite the expression for the muon neutrino flux, eq. (3), in the following form [18]:

$$\begin{aligned} \frac{F_\mu}{F_\mu^0} &\approx 1 - \sin^2 2\theta_{23} \sin^2 \frac{\phi}{2} \\ &\quad - \frac{1}{2} \sin^2 2\theta_{23} \cos \phi [1 - \text{Re}(A_{22}^* A_{33})] \\ &\quad - \left(s_{23}^4 - \frac{s_{23}^2}{r} \right) \tilde{P}_A - \left(c_{23}^4 - \frac{c_{23}^2}{r} \right) \tilde{P}_S \\ &\quad - \sin 2\theta_{23} P_\delta, \end{aligned} \quad (7)$$

where

$$\tilde{P}_A \equiv |A_{e\tilde{3}}|^2 \quad \text{and} \quad \tilde{P}_S \equiv |A_{e\tilde{2}}|^2 \quad (8)$$

are the probabilities of transitions $\nu_e \rightarrow \tilde{\nu}_2$ and $\nu_e \rightarrow \tilde{\nu}_3$ correspondingly, and P_δ is the function which depends on the CP-violation phase δ . In eq. (7) ϕ is the oscillation phase due to the 2-3 mass splitting: $\phi = \Delta m_{32}^2 x / 2E$, $c_{23} \equiv \cos^2 \theta_{23}$, *etc.*. Notice that \tilde{P}_S , \tilde{P}_A , P_δ and ϕ do not depend on θ_{23} .

In eq. (7) the first two terms are due to vacuum oscillations driven by the 2-3 mixing and mass splitting; the second line describes interference of the 2-3 and 1-2 modes of oscillations. The product of amplitudes in this term can be approximated as

$$|A_{2\bar{2}}A_{3\bar{3}}| \approx \sqrt{(1 - \tilde{P}_A)(1 - \tilde{P}_S)}. \quad (9)$$

The terms in the third line describe effects of oscillations due to the 1-2 and 1-3 mixing. The last term in (7) describes the CP-violation. The leading (second) term as well as the interference and CP-violating terms are symmetric with respect to change of sign of the deviation: $\delta_{23} \rightarrow -\delta_{23}$. The octant symmetry (degeneracy) is broken by the terms in the third line of eq. (7); these terms vanish for the maximal 2-3 mixing and $r = 2$.

For antineutrinos one obtains the same formula as in eq. (7) with substitution $\tilde{P}_S \rightarrow \tilde{P}_S$, $\tilde{P}_A \rightarrow \tilde{P}_A$ and $r \rightarrow \bar{r}$.

The octant effect can be characterized by the octant asymmetry defined as

$$\frac{\Delta^{oct} F_\mu}{F_\mu^0} \equiv \frac{1}{F_\mu^0} [F_\mu(45^\circ + \delta_{23}) - F_\mu(45^\circ - \delta_{23})]. \quad (10)$$

For such symmetric deviations from the maximal 2-3 mixing one has

$$\begin{aligned} \Delta(\sin^2 2\theta_{23}) &= 0, \\ \Delta(\cos^2 \theta_{23}) &= \Delta(\cos^4 \theta_{23}) = -\sin 2\delta_{23}. \end{aligned} \quad (11)$$

Then according to eq. (7) the octant asymmetry equals

$$\frac{\Delta^{oct} F_\mu}{F_\mu^0} = \sin 2\delta_{23} \left(1 - \frac{1}{r}\right) (\tilde{P}_A - \tilde{P}_S). \quad (12)$$

Notice that \tilde{P}_S and \tilde{P}_A enter the asymmetry with opposite signs, and therefore partly cancel each other.

To get an idea about dependences of the probabilities on the neutrino parameters one can use expressions for the amplitudes in medium with constant density:

$$\begin{aligned} A_{e\bar{e}} &= c_{13}^m \sin 2\theta_{12}^m \sin \phi_{21}^m, \\ A_{e\bar{3}} &= \sin 2\theta_{13}^m \left(\sin \phi_{32}^m e^{-i\phi_{31}^m} + \cos^2 \theta_{12}^m \sin \phi_{21}^m \right) \end{aligned} \quad (13)$$

The probability $\tilde{P}_S \propto \sin^2 2\theta_{12}^m$ decreases with energy, whereas $\tilde{P}_A \propto \sin^2 2\theta_{13}^m$ increases being resonantly enhanced in the neutrino channel (for the normal mass hierarchy) at high energies. Here sensitivity of ICAL to the sign of muon charge will play important role. The two probabilities become comparable at 1 GeV for $\sin^2 \theta_{13} \sim 0.01$.

In the limit of zero 1-3 mixing $\tilde{P}_A = 0$, $\tilde{P}_S \rightarrow P_S$, and one finds from eq. (7)

$$\begin{aligned} \frac{F_\mu}{F_\mu^0} &\approx 1 - \sin^2 2\theta_{23} \sin^2 \frac{\phi}{2} - \frac{1}{2} \sin^2 2\theta_{23} \cos \phi \times \\ &\times \left(1 - \sqrt{1 - P_S}\right) - \left(c_{23}^4 - \frac{c_{23}^2}{r}\right) P_S, \end{aligned} \quad (14)$$

where $P_S = \tilde{P}_S(\theta_{13} = 0)$, which is the 2ν probability of oscillations driven by Δm_{21}^2 and θ_{12} . For the octant asymmetry we obtain

$$\frac{\Delta^{oct} F_\mu}{F_\mu^0} = -\sin 2\delta_{23} \left(1 - \frac{1}{r}\right) P_S. \quad (15)$$

At low energies: $r \approx 2$, and therefore the asymmetry equals $\sim 1/2 \sin 2\delta_{23} P_S$.

In fig. 1 we show the oscillograms for the octant asymmetry, that is, the lines of equal asymmetry $\Delta^{oct} F_\mu / F_\mu^0$ in the $E - \cos \theta_Z$ plane in neutrino and antineutrino channels. According to eq. (15) these oscillograms coincide with the oscillograms for P_S up to coefficient which weakly depends on E and θ_Z at $E < 1$ GeV. We use $\delta_{23} = 5^\circ$, $\theta_{13} = 0$, and other parameters are set at their best-fit values. The asymmetry increases with decrease of the neutrino energy. Maximal asymmetry is achieved in the 1-2 resonance ($E \sim 0.1$ GeV): $\Delta^{oct} F_\mu / F_\mu^0 \approx 0.087$. For realistic threshold $E_{th} = 0.3$ GeV and $\delta_{23} = 5^\circ$ the averaged asymmetry is about (2 - 3)% and for $E_{th} = 0.8$ GeV it is below 1%.

Notice that the octant asymmetry of ν_e -flux is about 4 times larger than the ν_μ -flux asymmetry:

$$\frac{\Delta^{oct} F_e}{F_e^0} = -\sin 2\delta_{23} r P_S. \quad (16)$$

Here, however, the original ν_e -flux is 2 times smaller. Furthermore, detection of muons provide better energy and direction resolutions.

Since P_S and \tilde{P}_S are of the same order, separation of the neutrino and antineutrino signals has no sense here.

Let us consider variations of the ν_μ -flux due to deviation of the 2-3 mixing from maximal. According to (7) the relative change of the flux, which we will call the θ_{23} -deviation effect, equals

$$\begin{aligned} \frac{\Delta^{dev} F_\mu}{F_\mu^0} &\equiv \frac{F_\mu(45^\circ) - F_\mu(45^\circ - \delta_{23})}{F_\mu^0} \approx \\ &- \Delta(\sin^2 2\theta_{23}) \sin^2 \frac{\phi}{2} \cong -\frac{1}{2} \sin^2 2\delta_{23}, \end{aligned} \quad (17)$$

where in the last equality we have averaged the oscillations due to large mass splitting.

Ratio of the octant asymmetry and the 2-3 deviation effect equals

$$\frac{\Delta^{oct} F_\mu}{\Delta^{dev} F_\mu} = -\frac{1}{\sin 2\delta_{23}} \left(1 - \frac{1}{r}\right) (\langle \tilde{P}_A \rangle - \langle \tilde{P}_S \rangle), \quad (18)$$

where $\langle \tilde{P}_S \rangle$ and $\langle \tilde{P}_A \rangle$ are the probabilities averaged over the experimental $E - \cos \theta_Z$ ranges. Although $\Delta^{dev} F_\mu^0$ is proportional to square of the deviation parameter, for not very small δ_{23} ($> 5^\circ$) and $\theta_{13} = 0$, the integral effect of the deviation from maximal mixing is stronger than the effect of octant. The reason is that the deviation effect does not change with energy, whereas the octant asymmetry being proportional to P_S quickly decreases with E ($\langle \tilde{P}_S \rangle \ll \langle \tilde{P}_A \rangle$). For zero 1-3 mixing and $\delta_{23} = 5^\circ$ we have $\Delta^{dev} F_\mu / F_\mu^0 = 0.015$, and $\Delta^{oct} F_\mu / F_\mu^0 = 0.087 \langle P_S \rangle$.

For non-zero 1-3 mixing at high energies the ratio of the flux differences is

$$\frac{\Delta^{oct} F_\mu}{\Delta^{dev} F_\mu} \cong -\left(1 - \frac{1}{r}\right) \frac{\langle \tilde{P}_A \rangle}{\sin 2\delta_{23}}, \quad (19)$$

and since \tilde{P}_A does not decrease with energy the ratio is not small in contrast to the previous case.

In our studies of sensitivities to the parameters of 2-3 sector we obtain the oscillation probabilities solving numerically full three flavor evolution equation and using the Preliminary Reference Earth Model (PREM) [19] for the density profile of the Earth. We will use the consideration presented in this section for interpretation of the numerical results.

III. THE χ^2 ANALYSIS FOR ICAL

To evaluate physics potential of the atmospheric neutrino studies with a magnetized ICAL detector we generated the atmospheric neutrino events and considered the muon energy and direction (directly measurable quantities) using event generator NUANCE-v3 [20]. The GEANT [21] simulation of ICAL detector shows that the energy and angular resolutions of muons are very high and the corresponding uncertainties are negligible compared to differences between the angles as well as energies of the neutrino and muon in the scattering (production) process.

χ^2 is calculated according to the Poisson distribution. The term due to contribution of prior information on the oscillation parameters measured by other experiments is not added to χ^2 here for conservative estimation; the effect of priors will be considered in sec. V. The data have been binned in cells of equal size in the $(\log_{10} E - L^{0.4})$ plane, where $L = 2R \cos \theta_Z$

is the length of neutrino trajectory. Choice of this binning is motivated by pattern of the oscillation probability $P(\nu_\mu \rightarrow \nu_\mu)$ in the $L - E$ plane [22]. The distance between two consecutive oscillation peaks in this plane increases (decreases) as one goes to lower L (E) values for a given E (L). The binning of L has been optimized to get better sensitivity to the oscillation parameters. To maintain $\chi^2/d.o.f. \approx 1$ in Monte Carlo simulation study, number of events should be > 4 per cell [17]. If the number is smaller than 4 (which happens in the high energy bins), we combine results from the nearest cells.

For each set of oscillation parameters we integrate the atmospheric neutrino flux at the detector over the energy and zenith angle folding it with the cross-section, the exposure time, the target mass, the efficiency of detection and the two dimensional energy-angle correlated resolution functions to obtain data for the χ^2 analysis. We use the charge current cross section of NUANCE-v3 [20] and the neutrino flux of the 3-dimensional scheme [23].

The systematic uncertainties of the atmospheric neutrino flux are crucial for determination of the oscillation parameters. We have divided them into two categories: (i) the overall flux normalization uncertainties which are independent of the neutrino energy and zenith angle, and (ii) the spectral tilt uncertainties which depend on E and θ_Z . The flux with uncertainties included can be written as

$$\Phi(E, \theta_Z) = \Phi_0(E) \left[1 + \delta_E \log_{10} \frac{E}{E_0}\right] \times [1 + \delta_Z (|\cos \theta_Z| - 0.5)] \times [1 + \delta_{f_N}]. \quad (20)$$

For $E < 1$ GeV we take the energy-dependent uncertainty: $\delta_E = 15\%$ and $E_0 = 1$ GeV, and for $E > 10$ GeV correspondingly, $\delta_E = 5\%$ and $E_0 = 10$ GeV. The uncertainty is $\delta_E \sim 7\%$ in the range $E = 1 - 10$ GeV. The overall flux uncertainty as function of the zenith angle is parameterized by δ_Z . According to [23] we use $\delta_Z = 4\%$ which leads to 2% vertical/horizontal flux uncertainty. We take for the overall flux normalization uncertainty $\delta_{f_N} = 10\%$ and for the neutrino cross-section uncertainty: $\delta_\sigma = 10\%$.

In our χ^2 analysis the numbers of events have been computed for the theoretical (fit) values and experimental (true) values of parameters in the same way by migrating the number of events from the neutrino to muon energy and zenith angle bins. The resolution functions have been taken from the previous work [24].

In studies of sensitivity to the 2-3 mixing we marginalize χ^2 over Δm_{32}^2 , θ_{13} , δ_{CP} for ν 's and $\bar{\nu}$'s separately. Then we find the total χ^2 as $\chi^2 = \chi_\nu^2 + \chi_{\bar{\nu}}^2$. We have chosen the following benchmark values of

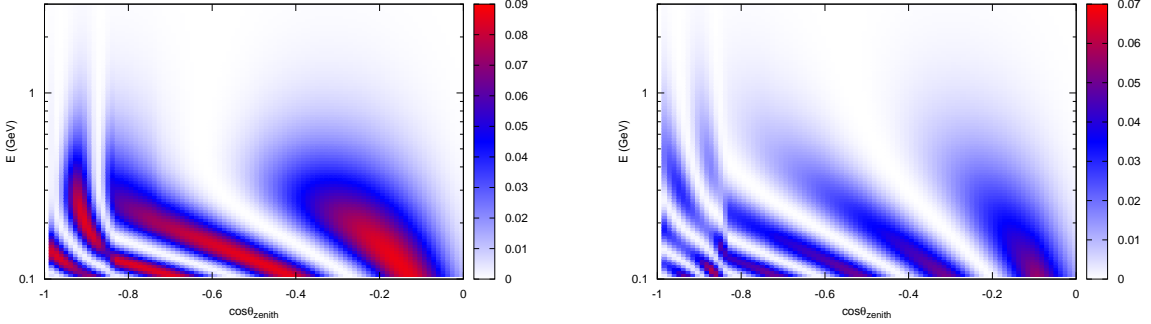


FIG. 1: The oscillograms for the octant asymmetry: The contours of equal asymmetry $\Delta^{oct} F_\mu / F_\mu^0$ for neutrino (left) and antineutrino (right) with $\delta_{23} = 5^\circ$ at $\theta_{13} = 0$. The other parameters are set at their best-fit values.

the neutrino parameters: $\Delta m_{32}^2 = 2.5 \times 10^{-3} \text{ eV}^2$, $\delta_{CP} = 0$, $\Delta m_{21}^2 = 7.9 \times 10^{-5} \text{ eV}^2$ and $\theta_{12} = 34.24^\circ$. In marginalization we use, first, flat distributions of values of the parameters in the following ranges: $\Delta m_{32}^2 = (2.3 - 2.7) \times 10^{-3} \text{ eV}^2$, $\theta_{23} = 36^\circ - 54^\circ$ and $\theta_{13} = 0^\circ - 10.5^\circ$. The range of θ_{13} is changed for some particular analyses. (The non-flat distributions of parameters will be considered in sec. V.)

The parameters Δm_{21}^2 and θ_{12} produce subleading effects on the atmospheric neutrino fluxes for $E > 1 \text{ GeV}$. Moreover, effect of these parameters in marginalization is very small due to their narrow allowed regions. Therefore we have taken fixed values of Δm_{21}^2 and θ_{12} in our analysis.

IV. SENSITIVITIES OF ICAL

In our computations we explored the neutrino energy range (0.141 -15) GeV, we used different energy thresholds and different exposures, \mathcal{E} , of 0.25, 1, 2, and 4 Mton·yr.

A. Determination of 2-3 mixing for $\theta_{13} = 0$

The sensitivity of ICAL experiment to θ_{23} is shown in fig. 2. We plot

$$\Delta\chi^2 \equiv \chi^2(\theta_{23}) - \chi^2(\theta_{23}^{true}) \quad (21)$$

as function of the fit value for fixed input values $\theta_{23}^{true} = 37^\circ$, (left) and 40° (right) with $\mathcal{E} = 1, 2$, and 4 Mton·yr. We have marginalized χ^2 with respect to all the oscillation parameters except θ_{23} . The figure shows high sensitivity to the deviation δ_{23} : it would

be possible to discriminate between a given θ_{23} and maximal mixing at 99% C.L., if $|\delta_{23}| > 5^\circ$. For instance, after 1 Mton·yr the angle $\theta_{23} = 37^\circ$ can be distinguished from 45° at 8σ level.

The figure shows also low sensitivity of the experiment to the octant. Indeed, $\Delta\chi^2$ is higher in the right minima which correspond to the wrong octant. After 1 Mton·yr exposure the difference of $\Delta\chi^2$ in the true and wrong octants is smaller than 1. The difference becomes more than 2 (90% CL) only after 4 Mton·yrs. Identification of the octant becomes even more difficult for smaller δ_{23} . If $\delta_{23} = 5^\circ$, we find $\Delta\chi^2 = 1.2$ for $\mathcal{E} = 4 \text{ Mton·yr}$. This result can be readily seen from our analytical consideration in sec. II. The probability P_S averaged over the energy interval (0.14 - 15) GeV equals $\langle P_S \rangle \sim 0.02$, so that for $\delta_{23} = 8^\circ$: $\Delta^{oct} F_\mu / F_\mu^0 \sim 4 \cdot 10^{-3}$, whereas $\Delta^{dev} F_\mu / F_\mu^0 \sim 0.04$ - an order of magnitude larger. As we mentioned before, this big difference of sensitivities to the deviation and octant (degeneracy) is because the octant asymmetry is collected only at very low energies where P_S is unsuppressed, whereas whole energy range contributes to the sensitivity to the deviation δ_{23} .

The sensitivity to δ_{23} drops down substantially with decrease of δ_{23} . Reducing δ_{23} from 8° to 5° (compare the left and right panel of fig. 2) leads to decrease of the flux difference of eq. (17) by factor 2.5, and correspondingly, significance of discrimination from maximal mixing becomes 2σ (for $\mathcal{E} = 1 \text{ Mton·yr}$). Sensitivity to the octant at the 1σ level appears only if $\mathcal{E} > 4 \text{ Mton·yr}$.

In fig. 3 we show the marginalized $\Delta\chi^2$, calculated at the maximal mixing (fit value) for different

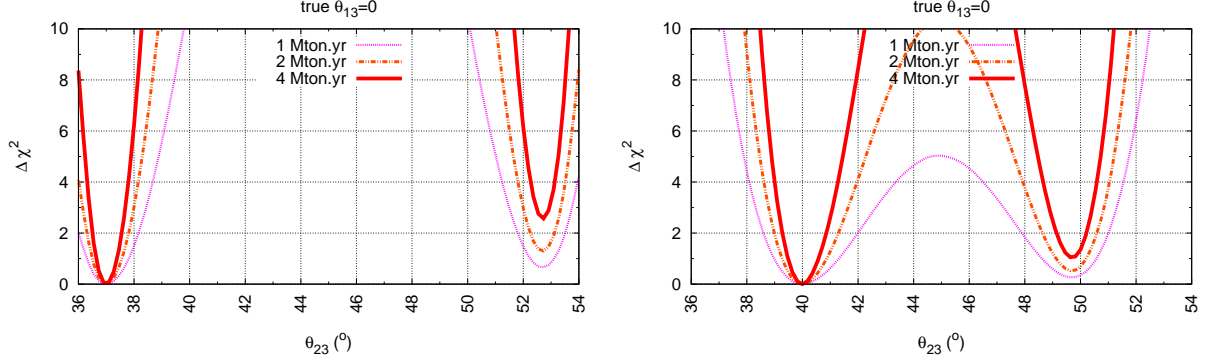


FIG. 2: Dependence of $\Delta\chi^2$ on fit value of θ_{23} for fixed input (true) values $\theta_{23} = 37^\circ$ (left) and 40° (right). We used $\theta_{13} = 0$, $\mathcal{E} = 1, 2$, and 4 Mton.yr, and the energy threshold 0.141 GeV. The χ^2 is marginalized with respect to all the oscillation parameters except θ_{23} . The range of marginalization for θ_{13} is $0 - 10.5^\circ$.

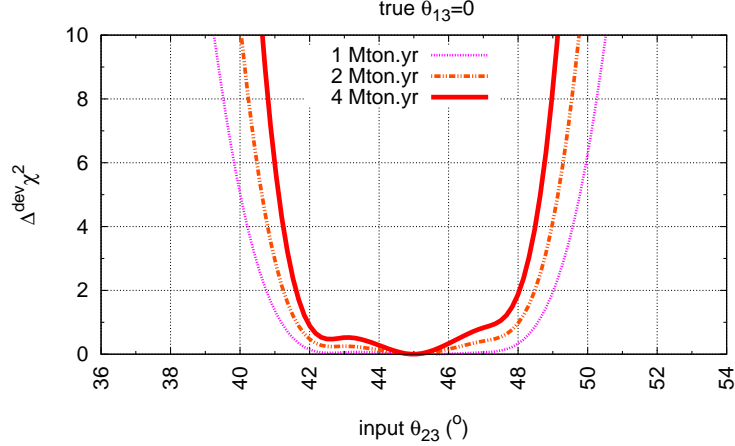


FIG. 3: Dependence of the ICAL sensitivity to the deviation from maximal mixing on the input value of θ_{23} for different exposure times: $\mathcal{E} = 1, 2$, and 4 Mton.yr. We use the threshold 0.141 GeV. Here $\Delta^{dev}\chi^2 = \chi^2(45^\circ) - \chi^2(\theta_{23}^{true})$. χ^2 is marginalized with respect to all the oscillation parameters except θ_{23} . The range of marginalization for θ_{13} is $0 - 10.5^\circ$.

input (true) values of θ_{23} :

$$\Delta^{dev}\chi^2 \equiv \chi^2(45^\circ) - \chi^2(\theta_{23}^{true}). \quad (22)$$

The picture is complementary to that in fig. 2, and there is an approximate symmetry with respect to $\theta_{23} = 45^\circ$. The reason of sharp increase of $\Delta\chi^2$ at 42 and 48° is related to weak dependence of the oscillation probability on $\delta_{23} = 0$ around $\delta_{23} = 0$ and to overall flux uncertainty.

In fig. 4 we illustrate dependence of the sensitivity to the octant on θ_{23} . For different input (true) values of θ_{23} we plotted

$$\Delta^{oct}\chi^2 \equiv \chi^2(90^\circ - \theta_{23}) - \chi^2(\theta_{23}). \quad (23)$$

According to fig. 4, it will be possible to discriminate the octant at 90% CL if $\theta_{23} \lesssim 38^\circ$ or $\gtrsim 52^\circ$ after $\mathcal{E} = 4$ Mton.yr. Notice that the curves are nearly symmetric with respect to $\theta_{23} = 45^\circ$.

Due to fast decrease of P_S with increase of energy (see fig. 1) the sensitivity to the octant disappears for high values of the threshold.

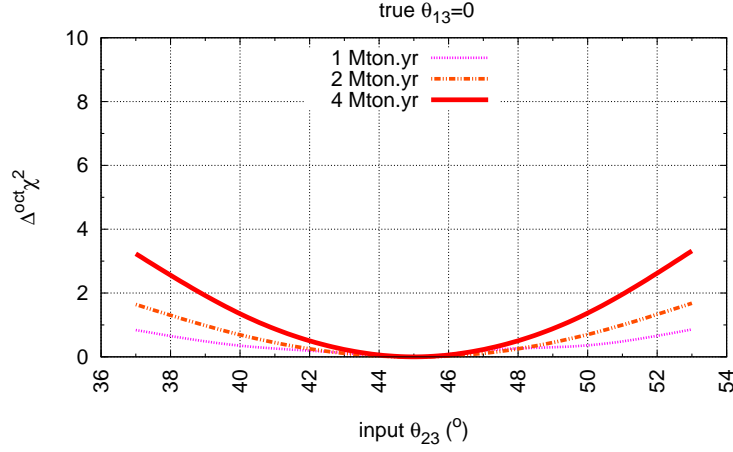


FIG. 4: Dependence of the ICAL sensitivity to the θ_{23} -octant on the input (true) value of θ_{23} for different values of \mathcal{E} , and threshold 0.141 GeV. Here $\Delta^{\text{oct}}\chi^2 = \chi^2(90^\circ - \theta_{23}) - \chi^2(\theta_{23})$. χ^2 is marginalized with respect to all the oscillation parameters except θ_{23} . The range of marginalization for θ_{13} is $0 - 10.5^\circ$.

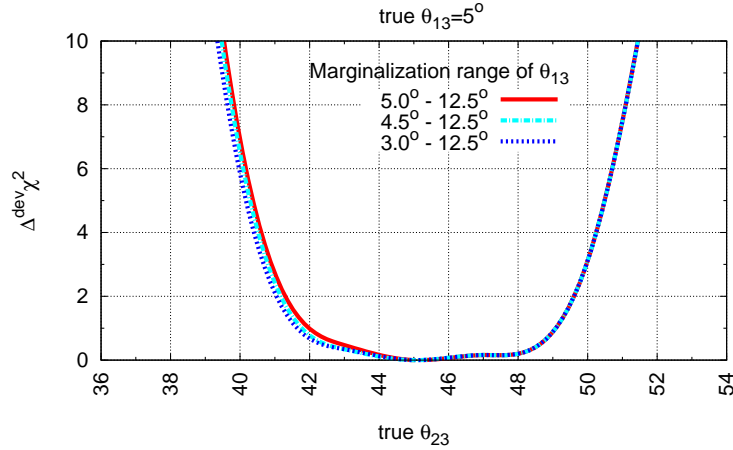


FIG. 5: Dependence of the ICAL sensitivity to the deviation from maximal 2-3 mixing on the input value of θ_{23} for different marginalization ranges of θ_{13} . We use $\mathcal{E} = 1$ Mton-yr and threshold 0.806 GeV. Here $\Delta^{\text{dev}}\chi^2 \equiv \chi^2(45^\circ) - \chi^2(\theta_{23}^{\text{true}})$. χ^2 is marginalized with respect to all oscillation parameters except θ_{23} .

B. Determination of θ_{23} in the presence of non-zero 1-3 mixing.

Analysis of the oscillation data testifies for the non-zero 1-3 mixing, although significance of this result is not high and zero value of θ_{13} is not yet excluded. The global fit at 1σ C.L. gives $\theta_{13} = 7.3^\circ \pm_{-3.2^\circ}^{+2.1^\circ}$, with 3σ upper bound of $\theta_{13} < 13^\circ$, and $\delta_{\text{CP}} \in [0, 360]$ [2]. Analysis of the solar and KAMLAND data by SNO collaboration leads to $\theta_{13} =$

$8.13^\circ \pm_{-7.03^\circ}^{+3.53^\circ}$ at 95% CL [25]. New and forthcoming experiments Double Chooz, Daya Bay, RENO, T2K, NO ν A can confirm this result with higher confidence level or put new stringent upper bound [26] which would correspond approximately to a situation with zero 1-3 mixing considered in the previous section.

By the time when ICAL will collect significant statistics the angle θ_{13} will be known with relatively good accuracy. To clarify an impact of this information on the determination of parameters of the 2-3

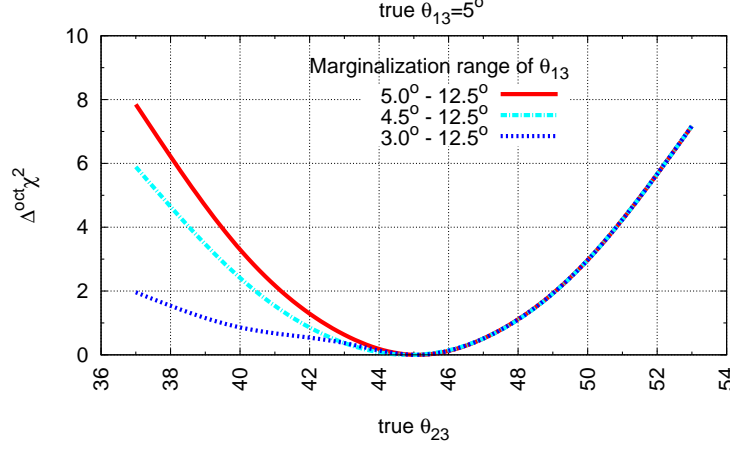


FIG. 6: Dependence of the ICAL sensitivity to the θ_{23} -octant on the input value of θ_{23} with $\mathcal{E} = 1$ Mton-yr and threshold of 0.806 GeV. Here $\Delta^{\text{oct}}\chi^2 \equiv \chi^2(90^\circ - \theta_{23}) - \chi^2(\theta_{23})$. χ^2 is marginalized with respect to all oscillation parameters except θ_{23} .

sector we have performed analysis for non-zero θ_{13} . For illustration purpose we use $\theta_{13} = 5^\circ$ as the true value and different fit intervals with flat distribution (which could reflect errors in measurements of θ_{13}).

In fig. 5 we show dependence of $\Delta^{\text{dev}}\chi^2$ defined in eq. (22) on the true (input) value of θ_{23} for the fit value $\theta_{23} = 45^\circ$ and $\mathcal{E} = 1$ Mton-yr. Different curves correspond to different marginalization intervals of θ_{13} . Comparing these results with the results of fig. 3 we find that inclusion of the 1-3 mixing does not change significantly the sensitivity to δ_{23} . The reason is that this sensitivity follows from the main mode of the ν_μ -oscillations; large probability for this mode extends to higher energies and 1-3 mixing produces just additional distortion of the oscillatory pattern. However, inclusion of the 1-3 mixing makes the curve less symmetric with respect to 45° which reflects an increase of sensitivity to the octant. Also sensitivity to the deviation weakly depends on the marginalization interval for θ_{13} .

Fig. 6 illustrates the sensitivity of ICAL to the octant in the presence of non-zero 1-3 mixing. We show dependence of $\Delta^{\text{oct}}\chi^2$ defined in eq. (23) on the true value of $\theta_{23}^{\text{true}}$ for the fit value $\theta_{23}^{\text{fit}} = 90^\circ - \theta_{23}$. Different curves correspond to different marginalization intervals for θ_{13} . There are two important features of the fig. 6. First, the sensitivity to the octant is substantially better for non-zero value of θ_{13} than for vanishing 1-3 mixing (fig. 6) as was also shown in previous publications [13, 27–29]. This is related to the fact that the octant asymmetry of the flux is

determined now by

$$\frac{\Delta^{\text{oct}}F}{F_\mu^0} \approx \sin 2\delta_{23} \left(1 - \frac{1}{r}\right) \langle P_A \rangle \quad (24)$$

and $\langle P_A \rangle \sim 0.1$ in the interval $E = (0.14 - 15)$ GeV; it is much larger than $\langle P_S \rangle$ being enhanced in the energy range $E = (3 - 10)$ GeV (in the resonance channel). Furthermore, at high energies $r \sim (3 - 4)$ and value of the coefficient in eq. (24) becomes larger. As a result, for $\theta_{23} = 51^\circ$ the octant can be identified at 2σ level ($\Delta^{\text{oct}}\chi^2 = 4$) with $\mathcal{E} = 1$ Mton-yr, as compared to $\Delta^{\text{oct}}\chi^2 = 0.3$ for $\theta_{13} = 0$.

The second feature is significant asymmetry of the curves with respect to $\theta_{23} = 45^\circ$. The asymmetry is practically absent for fixed input value of θ_{13} but it increases with broadening of the marginalization interval, and more importantly, with increase of the lower border of this interval. For $\theta_{23} > 45^\circ$ the curves are practically not changed with change of the interval, whereas for $\theta_{23} < 45^\circ$ the sensitivity substantially decreases. For instance, taking $\theta_{23} = 40^\circ$ we obtain $\Delta\chi^2 = 1$ for the interval $\theta_{13} = (3^\circ - 12.5^\circ)$ instead of $\Delta^{\text{oct}}\chi^2 = 3$ for fixed value $\theta_{13} = 5^\circ$.

This asymmetry can be readily understood from the analytic consideration of sec. II. Neglecting the effect of 1-2 mixing the ν_μ -flux can be presented as

$$\frac{F_\mu}{F_\mu^0} \approx K(\sin 2\theta_{23}) - f(\theta_{23}) \left(1 - \frac{1}{r}\right) P_A(\theta_{13}), \quad (25)$$

where $K(\sin 2\theta_{23})$ is an even function of the deviation

(symmetric with respect to change of the octant), and

$$f(\theta_{23}) \equiv \left(s_{23}^4 - \frac{s_{23}^2}{r} \right) \quad (26)$$

quickly increases with θ_{23} , so that for $r = 3 - 4$ one has $f(\theta_{23} = 40^\circ) \ll f(\theta_{23} > 50^\circ)$. Therefore for $\theta_{23} < 45^\circ$ the flux F_μ has much weaker dependence on θ_{13} than for $\theta_{23} > 45^\circ$. In the process of marginalization over θ_{13} we compare the true value of the flux, F_μ^{true} , with the fit value, F_μ^{fit} , and $\Delta^{oct}\chi^2$ is proportional to their difference:

$$\frac{1}{F_\mu^0} |F_\mu^{true} - F_\mu^{fit}| = \left(1 - \frac{1}{r} \right) \times |f(\theta_{23}) \langle P_A(\theta_{13}^{true}) \rangle - f(90^\circ - \theta_{23}) \langle P_A(\theta_{13}) \rangle| \quad (27)$$

If the fit value of 1-3 mixing is fixed: $\theta_{13}^{fit} = \theta_{13}^{true}$, the curve is approximately symmetric with respect to change $\theta_{23} \leftrightarrow (90^\circ - \theta_{23})$. Indeed, in this case we have from eq. (27)

$$\frac{1}{F_\mu^0} |F_\mu^{true} - F_\mu^{fit}| = \left(1 - \frac{1}{r} \right) \times \langle P_A(\theta_{13}^{true}) \rangle |f(\theta_{23}) - f(90^\circ - \theta_{23})|. \quad (28)$$

The situation is different if θ_{13} varies in certain interval $\theta_{13} = [\theta_{13}^{min} - \theta_{13}^{max}]$, and we perform marginalization over θ_{13} in this interval. Marginalization minimizes the difference of fluxes (eq. (27)) over θ_{13} for a given value of θ_{23} . If $\theta_{23} < 45^\circ$, then $f(\theta_{23}) \ll f(90^\circ - \theta_{23})$. In this case the difference of fluxes is minimal if $\theta_{13} \sim \theta_{13}^{min}$. Indeed, since $\langle P_A \rangle$ decreases with θ_{13} , a small value of $\langle P_A \rangle$ partially compensates large value of $f(90^\circ - \theta_{23})$ in the second term on the right hand side of eq. (27). Furthermore, the smaller θ_{13}^{min} the stronger compensation, and therefore the smaller $\Delta\chi^2$ can be obtained. If $\theta_{23} > 45^\circ$, then $f(\theta_{23}) \gg f(90^\circ - \theta_{23})$. Now to compensate the first term in eq. (27) one should take $\langle P_A(\theta_{13}^{fit}) \rangle \gg \langle P_A(\theta_{13}) \rangle$. This is, however, not possible for the considered values of θ_{13} . Thus, in the case of unprecise determination of θ_{13} sensitivity to the octant is higher for $\theta_{23} > 45^\circ$.

C. Determination of the 2-3 mass split. CPT test

Important advantage of a magnetized calorimeter is that it allows one to measure the neutrino mass differences and mixing angles in the neutrino and antineutrino channel separately. A difference of results can be related to some effective or fundamental violation of the CPT symmetry.

In fig. 7 we show dependence of $\Delta\chi^2$ on the fit value of Δm_{32}^2 for the true value $\Delta m_{32}^2 = 2.35 \cdot 10^{-3} \text{ eV}^2$ in the neutrino and antineutrino channels. We take $\theta_{13} = 5^\circ$ and $\theta_{23} = 45^\circ$. According to this figure with $\mathcal{E} = 0.25 \text{ Mton}\cdot\text{yr}$ the value $\Delta m_{32}^2 = 3.3 \cdot 10^{-3} \text{ eV}^2$ can be discriminated from the true value at about 2σ level.

The accuracy of measurement of Δm_{32}^2 is better in the ν -channel. For $\mathcal{E} = 0.25 \text{ Mton}\cdot\text{yr}$ the error in ν -channel is about two times smaller than that in $\bar{\nu}$ channel. The difference of accuracies decreases with increase of exposure and e.g. for $1 \text{ Mton}\cdot\text{yr}$ it becomes about 25%. The curves $\Delta\chi^2$ are asymmetric with respect to $\Delta m_{32}^{2, true}$, which is related to the dependence of oscillation probability on Δm_{32}^2 .

The 1σ error for Δm_{32}^2 could be $0.15 \cdot 10^{-3} \text{ eV}^2$ and $0.04 \cdot 10^{-3} \text{ eV}^2$ after $0.25 \text{ Mton}\cdot\text{yr}$ and $1 \text{ Mton}\cdot\text{yr}$ exposures correspondingly. With $\mathcal{E} = 1 \text{ Mton}\cdot\text{yr}$ the error $0.15 \cdot 10^{-3} \text{ eV}^2$ can be achieved at 3σ level. With $\mathcal{E} = 1 \text{ Mton}\cdot\text{yr}$ one can obtain an accuracy $0.08 \cdot 10^{-3} \text{ eV}^2$ (90% C.L.) which is better than the present MINOS accuracy.

In figs. 8 and 9 we show $\Delta\chi^2$ as function of Δm_{32}^2 and θ_{23} in the neutrino and antineutrino channels for $\mathcal{E} = 0.25$ and $1 \text{ Mton}\cdot\text{yr}$. As true values we take $\theta_{23} = 45^\circ$ and $\Delta m_{32}^2 = 2.35 \cdot 10^{-3} \text{ eV}^2$. According to fig. 9 the present MINOS result for $\bar{\nu}$ ($|\Delta m_{31}^2| = 3.36 \cdot 10^{-3} \text{ eV}^2$, $\theta_{23} = 34^\circ$) can be excluded by ICAL at about 6σ level with $\mathcal{E} = 1 \text{ Mton}\cdot\text{yr}$.

V. FURTHER IMPROVEMENTS OF SENSITIVITIES

There are several directions in which sensitivity of ICAL can be further improved.

A. Adding information about hadrons

Measurements of the hadron energy in ICAL in addition to the muon energy is expected to improve reconstruction of the neutrino energy for $E \gtrsim 2 \text{ GeV}$. However, the total hadron energy in an event is carried out by multiple low energy hadrons. The average energy per hadron per event is $\lesssim 1 \text{ GeV}$ and the average number of hadrons per event is $\gtrsim 2$ At $E \lesssim 1 \text{ GeV}$ the energy resolution is very poor, roughly 80%, and the number of hits (number of active detector layers in which signal is detected) increases only logarithmically with E .

The resolution of hadron energy (for all pions and kaons) at ICAL has been obtained from GEANT4

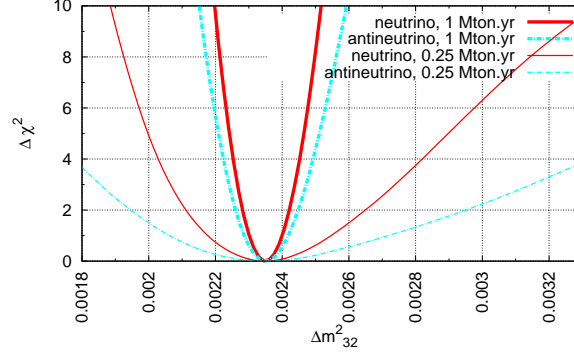


FIG. 7: Dependence of $\Delta\chi^2$ on the fit value of Δm_{32}^2 for the true value $\Delta m_{32}^2 = 2.35 \times 10^{-3} \text{ eV}^2$ in the neutrino and antineutrino channels. We use $\mathcal{E} = 0.25$ and 1 Mton.yr and the threshold 0.8 GeV. The marginalization is done over all the oscillation parameters except Δm_{32}^2 . The χ^2 values 1, 4, 9 correspond to 1σ (68.3%), 2σ (95.4%), and 3σ (99.73%), respectively.

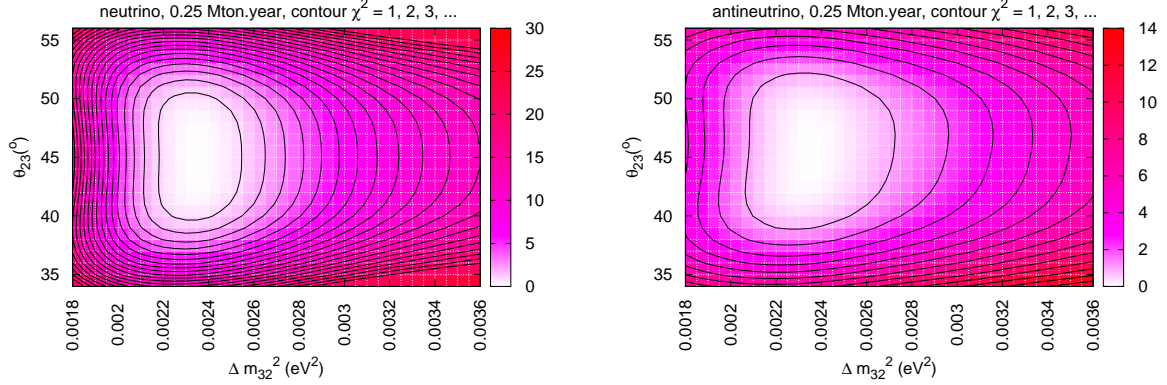


FIG. 8: The iso- χ^2 contours in the $\Delta m_{32}^2 - \theta_{23}$ plane for neutrinos (left) and antineutrinos (right) obtained with $\mathcal{E} = 0.25$ Mton.yr. The inner contour corresponds to $\chi^2 = 1$ and others with increment 1. We use the input value $\Delta m_{32}^2 = -2.35 \times 10^{-3} \text{ eV}^2$, $\theta_{23} = 45^\circ$, $\theta_{13} = 5^\circ$ and the threshold 0.8 GeV. Here $\Delta\chi^2$ values 2.3, 4.6, 9.2 correspond to 1σ (68.3%), 2σ (90%), and 3σ (99%), respectively. Intensity of color reflects value of $\Delta\chi^2$ (see column on the right hand sides of the panels for identification).

simulation and parametrized as

$$\sigma_{had}/E_{had} = a/\sqrt{E_{had}} + b, \quad (29)$$

where, $a \approx 0.60$ and $b \approx 0.1$ for the thickness of iron layer 5.6 cm and after averaging over all directions.

For each hadron in an event we find the reconstructed hadron energy (E_{had}^{rec}) by a random number method using the value of σ_{had} from eq. 29. Then we find the final resolution as a function of $[E_\nu - (E_\mu + E_{had}^{recS})]/E_\nu$; where, E_{had}^{recS} is the sum of the energies of all reconstructed hadrons in an event. We use the atmospheric neutrino events without oscillations for an exposure of $50 \times 1000 \text{ kTon.yr}$ generated by Nuance to reconstruct the resolution functions for

each energy and zenith angle bins.

In fig. 10 we show the iso- χ^2 contours with and without inclusion of information about hadrons. We find that improvement of the sensitivity to θ_{23} , and therefore δ_{23} , is marginal. Also there is a very small change in the sensitivity to Δm_{32}^2 : $\Delta(\Delta m_{32}^2) = 0.02 \cdot 10^{-3} \text{ eV}^2$.

B. Cross-sections and fluxes

Figs. 11 and 12 illustrate improvements of the sensitivities with reduction of different systematic un-

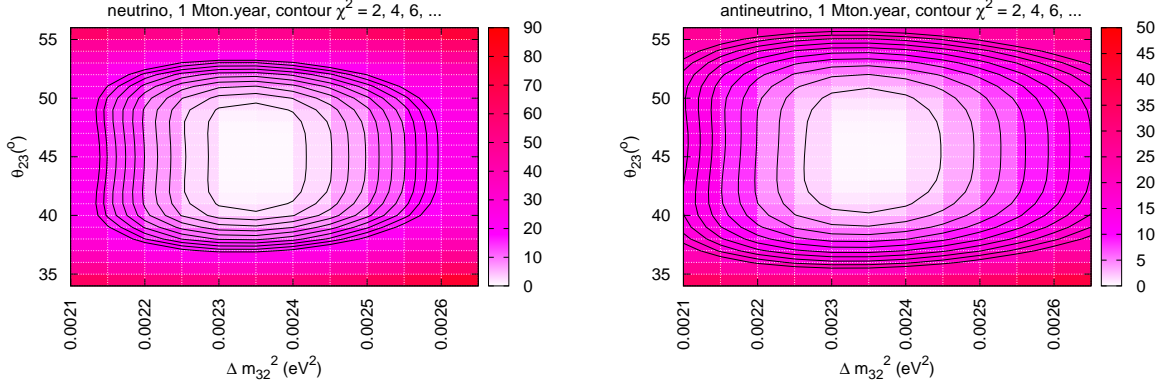


FIG. 9: The same as in fig. 8 but for $\mathcal{E} = 1$ Mton-yr. The inner contour corresponds to $\chi^2 = 2$ and for other contours the increment $\Delta\chi^2 = 2$.

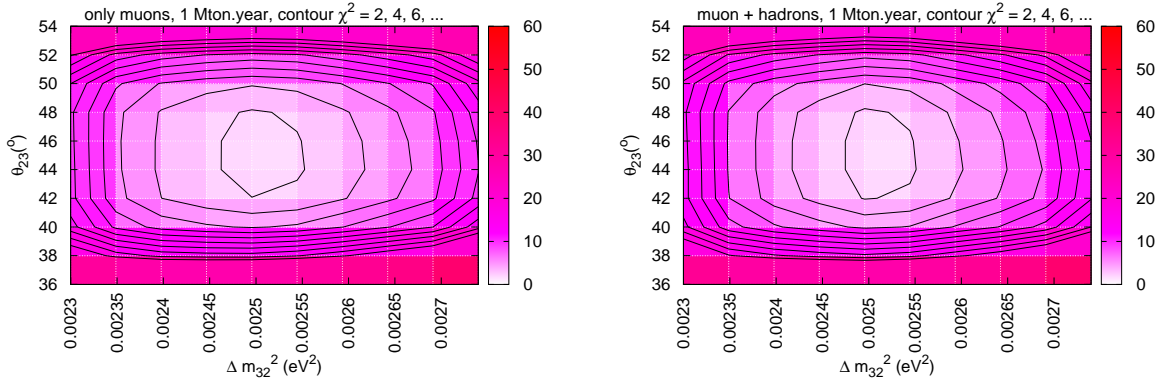


FIG. 10: Effect of inclusion in the analysis the information on hadrons. The iso- χ^2 contours (from inner side $\chi^2 = 2$ with increment 2) in the $\Delta m_{32}^2 - \theta_{23}$ plane without hadrons (left) and with hadrons (right). We take 1 Mton-yr, the threshold 0.8 GeV for both muons and hadrons. and sum up the signals from neutrinos and antineutrinos.

certainties. Decrease of uncertainties of the overall flux normalization, the ratio of horizontal/vertical flux, the neutrino cross-section, and the tilt (below 1 GeV) from 10%, 10%, 2%, and 15% to 2%, 2%, 2%, and 3%, respectively, do not lead to significant improvement of the sensitivities. The reason is that the up-going neutrinos oscillate and down-going neutrinos remain practically unchanged. In χ^2 analysis these down-going neutrinos allow to reduce the effect of systematic uncertainties in fluxes. Significant improvement occurs only when all systematic uncertainties are zero.

C. Adding priors to χ^2

In χ^2 analysis in sec. 4 for simplicity we used flat distributions of uncertainties of the oscillation param-

eters in marginalization. The prior contribution of the parameters to χ^2 should improve the sensitivity. Proper procedure would require the use of the best-fit values and variations of parameters (especially θ_{13}) which will be possible after results of forthcoming experiments will be known.

In figs. 13 and 14 we show improvements of the sensitivities to the θ_{23} deviation and the octant due to inclusion of the prior contribution. We have assumed the Gaussian distribution of the uncertainties around the best fit with width $\sigma(\sin^2 2\theta_{13}) = 0.01$, $\sigma(\sin^2 2\theta_{23}) = 0.015$ and $\sigma(\Delta m_{32}^2)/\Delta m_{32}^2 = 0.015$ following [30, 31]. The 2σ errors in measurements of Δm_{32}^2 are ± 0.09 with flat uncertainties of oscillation parameters, ± 0.07 with prior information from present global-fit, and ± 0.018 with prior information from possible T2K result.

The asymmetry in the sensitivity to the octant

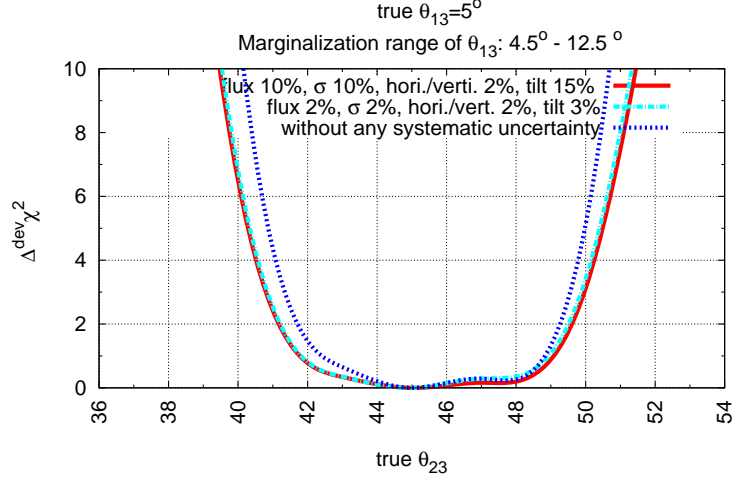


FIG. 11: The same as in fig. 5, but with reduced systematic uncertainties.

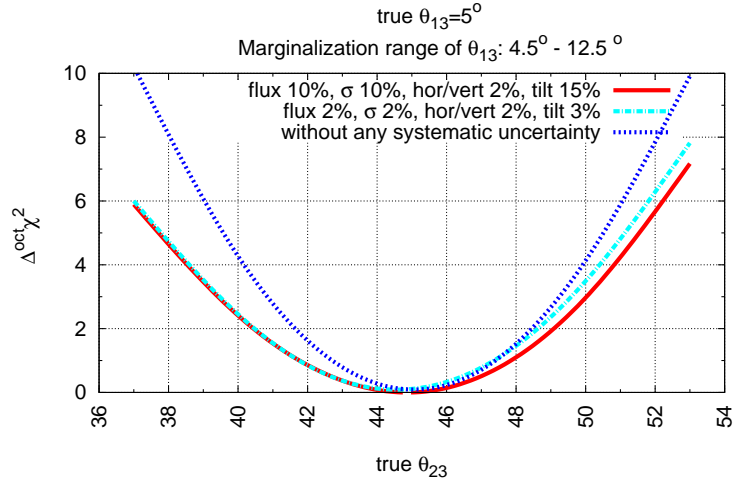


FIG. 12: The same as in fig. 6, but with reduced systematic uncertainties.

(which was due to the uncertainty of θ_{13} in absence of prior contribution) now disappears, and the result does not depend on marginalization range.

Of course, larger values of θ_{13} can substantially enhance the sensitivity to the octant since $P_A \sim \sin^2 \theta_{13}$ at low energies.

VI. CONCLUSION

We have studied analytically the dependence of the θ_{23} -deviation effect and octant asymmetry of ν_μ and $\bar{\nu}_\mu$ fluxes on the neutrino parameters θ_{23} and θ_{13} .

We explored numerically a sensitivities of a magnetized calorimeter to the θ_{23} -deviation, to the octant and to Δm_{32}^2 .

We show that for $\theta_{13} = 0$ the sensitivity of ICAL to the octant is low even for maximally allowed values of the deviation of the 2-3 mixing from maximal. This is related to the fact that the octant asymmetry is proportional to the “solar” probability P_S which is large: $O(1)$ at $E \sim 0.1$ GeV but quickly, as $\propto E^{-2}$, decreases with energy. The situation can be improved by lowering the threshold, increasing exposure and reducing systematic errors (especially in spectral index). We find that $sign(\delta_{23})$ (octant) can be established at 90% C.L. if $|\delta_{23}| = 7^\circ$, $\mathcal{E} = 4$ Mton·yr and

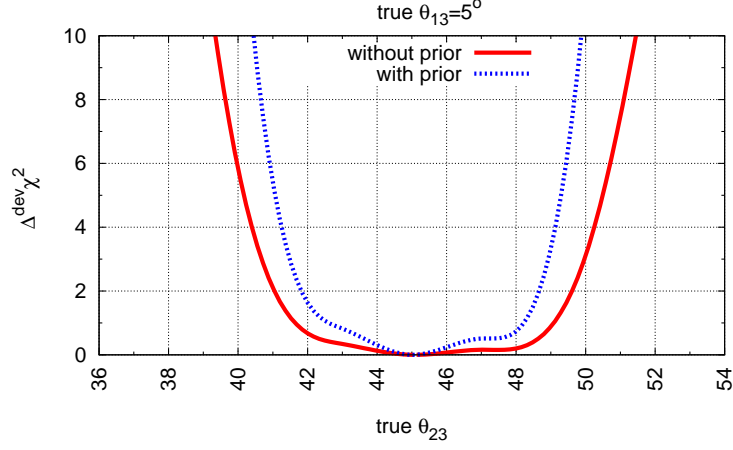


FIG. 13: The same as in fig. 5, but with the contributions from priors for the oscillation parameters added to χ^2 (see text). The marginalization range for θ_{13} is $3^\circ - 12.5^\circ$ ($0^\circ - 12.5^\circ$) in absence (presence) of prior contribution.

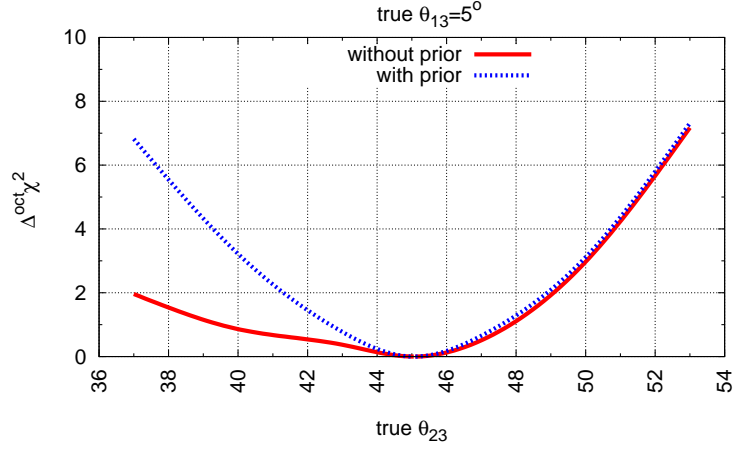


FIG. 14: The same as in fig. 6, but with the contribution from priors for the oscillation parameters added to the χ^2 . The marginalization range for θ_{13} is $3^\circ - 12.5^\circ$ ($0^\circ - 12.5^\circ$) in absence (presence) of prior contribution.

$E_{th} = 0.141$ GeV.

ICAL has good sensitivity to the θ_{23} -deviation from maximal 2-3 mixing: the effect is proportional to the probability of the main channel of oscillations, $\nu_\mu - \nu_\tau$, which is unsuppressed in whole considered neutrino energy range. As a result, dependence of the sensitivity on the energy threshold is weak and it does not change substantially when the effect of 1-3 mixing is included. We find that with the 1 Mton·yr exposure the 3σ accuracy of determination of the deviation will be $|\delta_{23}| \approx 6^\circ$, which is better than the present global fit result and slightly better than expected sensitivity

of T2K ($\approx 9^\circ$).

The oscillations driven by non-zero 1-3 mixing substantially improve the sensitivity to the octant. One can determine the octant for $\delta_{23} = 5^\circ$ and $\theta_{13} = 5^\circ$ at 90% C.L. with 1 Mton·yr exposure. We find that this sensitivity depends crucially on the uncertainty range of θ_{13} . For a given nonzero θ_{13} , the sensitivity to octant discrimination is symmetric in θ_{23} with respect to $\theta_{23} = 45^\circ$. However, the asymmetry arises (smaller sensitivity for $\theta_{23} < 45^\circ$) if value of θ_{13} can vary in large range. The symmetry is restored if prior for the 1-3 mixing is added.

TABLE I: Results of determination of θ_{23}

| θ_{23} | CL | Source |
|--|-----------|---------------------------|
| $42.9^{+4.1}_{-2.8}^\circ$ | 1σ | global-fit[2] |
| $35.7^\circ - 54^\circ$ | 3σ | global-fit[2] |
| $45^{+10}_{-7.8}^\circ$ | 99% | SK [4] |
| $45^\circ \pm 9^\circ$ | 90% | MINOS (ν) [4] |
| $34^{+6}_{-4}^\circ$ or $56^{+4}_{-6}^\circ$ | 90% | MINOS ($\bar{\nu}$) [5] |
| $39^\circ - 51^\circ$ | 2σ | T2K [32] |
| $36^\circ - 54^\circ$ | 2σ | NO ν A [32] |
| $40^\circ - 50^\circ$ | 2σ | INO (1 Mton-yr) |

TABLE II: Results of determination of Δm_{31}^2

| $\Delta m_{32}^2 (10^{-3} \text{eV}^2)$ | CL | Source |
|---|---------------|-----------------------|
| $-2.36 \pm 0.07 (\pm 0.36)$ | $1 (3)\sigma$ | global-fit [2] |
| $+2.47 \pm 0.12 (\pm 0.37)$ | $1 (3)\sigma$ | global-fit [2] |
| $2.5^{+0.52}_{-0.60}$ | 99% | SK 3ν [4] |
| $2.35^{+0.11}_{-0.08}$ | 90% | MINOS ν [5] |
| $3.36^{+0.45}_{-0.40}$ | 90% | MINOS $\bar{\nu}$ [5] |
| 2.5 ± 0.04 | 2σ | T2K [32] |
| $2.5^{+0.07}_{-0.04}$ | 2σ | NO ν A [32] |
| 2.5 ± 0.07 | 2σ | INO (1 Mton-yr) |

The accuracy of measurements of Δm_{23}^2 by ICAL, $\Delta(\Delta m_{23}^2) = 0.15 \cdot 10^{-3} \text{ eV}^2$ (3σ , 1 Mton-yr exposure), is two times better than the accuracy of the present global fit and it is worthier than the expected sensitivity of T2K.

ICAL can measure the difference of Δm_{32}^2 in ν and $\bar{\nu}$ channels (the CPT test) with accuracy $0.8 \times 10^{-4} \text{ eV}^2$ at 3σ confidence level with 1 Mton-yr exposure and the present MINOS result can be excluded at $> 5\sigma$ confidence level.

We find that inclusion of information about hadrons from neutrino interactions does not change the sensitivity to the oscillation parameters substantially. Also improvements of the sensitivity due to better determinations of the cross-section and neutrino flux are rather modest. However, the sensitivity improves substantially with adding priors, especially for the 1 - 3 mixing, and of course, with increase of the absolute value of 1-3 mixing.

Acknowledgments: The use of general cluster facility of Harish-Chandra Research Institute for a part of this work is gratefully acknowledged. A. S. wants to acknowledge Moon Moon Devi and Amol Dighe for providing the hadron resolution function.

-
- [1] R. N. Mohapatra and A. Y. Smirnov, Ann. Rev. Nucl. Part. Sci. **56**, 569 (2006) [arXiv:hep-ph/0603118]; and the reference there in.
- [2] M. C. Gonzalez-Garcia, M. Maltoni and J. Salvado, JHEP **1004**, 056 (2010) [arXiv:1001.4524 [hep-ph]].
- [3] G. L. Fogli, E. Lisi, A. Marrone, A. Palazzo and A. M. Rotunno, Phys. Rev. Lett. **101**, 141801 (2008) [arXiv:0806.2649 [hep-ph]].
- [4] J. Hosaka *et al.* [Super-Kamiokande Collaboration], Phys. Rev. D **74**, 032002 (2006) [arXiv:hep-ex/0604011].
- [5] P. Adamson *et al.* [The MINOS Collaboration], [arXiv:1103.0340 [hep-ex]].
- [6] J. Kopp, P. A. N. Machado and S. J. Parke, arXiv:1009.0014 [hep-ph].
- [7] V. Arumugam *et al.* [INO Collaboration], See, <http://www.imsc.res.in/ino/OpenReports/INOReport.pdf>
- [8] I. Kato [T2K Collaboration], J. Phys. Conf. Ser. **136**, 022018 (2008).
- [9] D. S. Ayres *et al.* [NO ν A Collaboration], [hep-ex/0503053].
- [10] C. W. Kim and U. W. Lee, Phys. Lett. B **444**, 204 (1998) [arXiv:hep-ph/9809491].
- [11] O. L. G. Peres and A. Y. Smirnov, Nucl. Phys. B **680**, 479 (2004) [arXiv:hep-ph/0309312].
- [12] O. L. G. Peres and A. Y. Smirnov, Phys. Rev. D **79**, 113002 (2009) [arXiv:0903.5323 [hep-ph]].
- [13] M. C. Gonzalez-Garcia, M. Maltoni and A. Y. Smirnov, Phys. Rev. D **70**, 093005 (2004) [arXiv:hep-ph/0408170].
- [14] S. Choubey and P. Roy, Phys. Rev. D **73**, 013006 (2006) [arXiv:hep-ph/0509197].
- [15] D. Indumathi, M. V. N. Murthy, G. Rajasekaran and N. Sinha, Phys. Rev. D **74**, 053004 (2006) [arXiv:hep-ph/0603264].
- [16] A. Bandyopadhyay *et al.* [ISS Physics Working Group], Rept. Prog. Phys. **72**, 106201 (2009) [arXiv:0710.4947 [hep-ph]].
- [17] A. Samanta, Phys. Rev. D **80**, 113003 (2009) [arXiv:0812.4639 [hep-ph]].
- [18] E. K. Akhmedov, M. Maltoni and A. Y. Smirnov, JHEP **0806**, 072 (2008) [arXiv:0804.1466 [hep-ph]].
- [19] A. M. Dziewonski and D. L. Anderson, Phys. Earth Planet. Interiors **25**, 297 (1981).

- [20] D. Casper, Nucl. Phys. Proc. Suppl. **112**, 161 (2002) [arXiv:hep-ph/0208030].
- [21] <http://geant4.web.cern.ch/geant4/>
- [22] A. Samanta, Phys. Rev. D **79**, 053011 (2009) [arXiv:0812.4640 [hep-ph]].
- [23] M. Honda, T. Kajita, K. Kasahara, S. Midorikawa and T. Sanuki, Phys. Rev. D **75**, 043006 (2007) [arXiv:astro-ph/0611418].
- [24] A. Samanta, Phys. Rev. D **81**, 037302 (2010) [arXiv:0907.3540 [hep-ph]].
- [25] B. Aharmim *et al.* [SNO Collaboration], Phys. Rev. C **81**, 055504 (2010) [arXiv:0910.2984 [nucl-ex]].
- [26] M. Mezzetto and T. Schwetz, J. Phys. G **37**, 103001 (2010) [arXiv:1003.5800 [hep-ph]].
- [27] K. Hiraide, H. Minakata, T. Nakaya, H. Nunokawa, H. Sugiyama, W. J. C. Teves, R. Zukanovich Funchal, neutrino oscillation experiments,” Phys. Rev. **D73**, 093008 (2006) [hep-ph/0601258].
- [28] T. Kajita, H. Minakata, S. Nakayama, H. Nunokawa, identical detectors with different baselines,” Phys. Rev. **D75**, 013006 (2007) [hep-ph/0609286].
- [29] D. Meloni, O. Mena, C. Orme, S. Palomares-Ruiz, S. Pascoli, JHEP **0807**, 115 (2008) [arXiv:0802.0255 [hep-ph]].
- [30] P. Huber, M. Lindner, T. Schwetz, W. Winter, JHEP **0911**, 044 (2009) [arXiv:0907.1896 [hep-ph]].
- [31] P. Huber, M. Lindner, M. Rolinec, T. Schwetz and W. Winter, Phys. Rev. D **70**, 073014 (2004) [arXiv:hep-ph/0403068].
- [32] P. Huber, M. Lindner, M. Rolinec, T. Schwetz and W. Winter, Nucl. Phys. Proc. Suppl. **145**, 190 (2005) [arXiv:hep-ph/0412133].